Ataxia telangiectasia mutated in cardiac fibroblasts regulates doxorubicin-induced cardiotoxicity

Hong Zhan[1,2], Kenichi Aizawa[1,2], Junqing Sun[2,4], Shota Tomida[1,2], Kinya Otsu[5], Simon J. Conway[6], Peter J. McKinnon[7], Ichiro Manabe[2], Issei Komuro[2], Kiyoshi Miyagawa[3], Ryozo Nagai[1], Toru Suzuki[1,2,8,9,*]

[1]Jichi Medical University, Tochigi, JAPAN

[2]Department of Cardiovascular Medicine, The University of Tokyo, Tokyo, JAPAN

[3]Department of Radiation Biology, Graduate School of Medicine, The University of Tokyo, Tokyo, JAPAN

[4]The Key Laboratory of Biomedical Information Engineering, Xi'an Jiaotong University, Xi'an, CHINA

[5]Cardiovascular Division, King's College London, London, UK

[6]Program in Developmental Biology and Neonatal Medicine, Herman B. Wells Center for Pediatric Research, Indiana University School of Medicine, Indianapolis, IN, USA

[7]Department of Genetics, St Jude Children's Research Hospital, Memphis, TN, USA

[8]Department of Cardiovascular Sciences, University of Leicester, Leicester, UK

[9]National Institute for Health Research Leicester Cardiovascular Biomedical Research Unit, Glenfield Hospital, Leicester, UK

*Address for correspondence: Toru Suzuki, Professor/Chair of Cardiovascular Medicine, Department of Cardiovascular Sciences, University of Leicester, Cardiovascular Research Centre, Glenfield Hospital, Groby Road, Glenfield, Leicester LE3 9QP United Kingdom. Tel; 0116 287 4741, Fax; 0116 287 5792, E-mail; ts263@le.ac.uk or torusuzu-tky@umin.ac.jp

Abstract

Aims: Doxorubicin (Dox) is a potent anti-cancer agent which is widely used in the treatment of a variety of cancers but its usage is limited by cumulative dose-dependent cardiotoxicity mainly due to oxidative damage. Ataxia telangiectasia mutated (ATM) kinase is thought to play a role in mediating the actions of oxidative stress. Here, we show that ATM in cardiac fibroblasts is essential for Dox-induced cardiotoxicity.

Methods and results: ATM knockout mice showed attenuated Dox-induced cardiotoxic effects (e.g. cardiac dysfunction, apoptosis, mortality). As ATM was expressed and activated predominantly in cardiac fibroblasts, fibroblast-specific *Atm*-deleted mice ($Atm^{fl/fl}$;*Postn-Cre*) were generated to address cell-type specific effects which showed that the fibroblast is the key lineage mediating Dox-induced cardiotoxicity through ATM. Mechanistically, ATM activated the Fas ligand, which subsequently regulated apoptosis in cardiomyocytes at later stages. Therapeutically, a potent and selective inhibitor of ATM, KU55933, when administered systemically was able to prevent Dox-induced cardiotoxicity.

Conclusion: ATM-regulated effects within cardiac fibroblasts are pivotal in Dox-induced cardiotoxicity, and antagonism of ATM and its functions may have potential therapeutic implications.

Key words: Doxorubicin, ataxia telangiectasia mutated, cardiac fibroblasts, doxorubicin-induced cardiotoxicity

Abbreviations: ATM=Ataxia telangiectasia mutated; Dox= doxorubicin; FasL=Fas ligand;

NAC=N-acetyl-L-cysteine

Short title: Role of ATM in cardiac fibroblasts on Dox-induced cardiotoxicity

Classifications: Heart failure

Translational Perspective

Doxorubicin is a widely used anti-cancer chemotherapeutic agent; however, its use is limited by

cumulative dose-dependent cardiotoxic effects which eventually lead to severe heart failure and

death. The present study demonstrates that ATM is a signaling molecule of oxidative stress

which mediates the cardiotoxic effects of doxorubicin in a murine model. The cell type-specific

mechanism that the cardiac fibroblast is the main lineage that mediates cardiotoxic effects

through ATM was identified. Moreover, a selective inhibitor of ATM, KU55933, was able to

prevent cardiotoxic effects. In perspective, ATM-regulated effects within cardiac fibroblasts are

pivotal in doxorubicin-induced cardiotoxicity, and antagonism of ATM and its functions may

have potential therapeutic implications.

Introduction

Doxorubicin (Dox) is a widely used anti-cancer chemotherapeutic agent. Unfortunately, its use

is also limited by cumulative dose-dependent cardiotoxic effects which lead to cardiac

dysfunction, cardiomyopathy, and eventually severe heart failure and death.[1] Although the

precise mechanisms underlying Dox-induced cardiotoxicity are not completely understood, most

studies favor that free radical-induced oxidative stress plays a pivotal role, as Dox possesses a

chemical structure that generates reaction oxygen species (ROS) during drug metabolism. Most

studies both *in vitro* and *in vivo* suggest that Dox-induced cardiotoxicity is associated with cardiomyocyte apoptosis and necrosis.[2-5]

Ataxia telangiectasia mutated (ATM) kinase is a member of the phosphoinositide 3-kinase (PI3-kinase)-related protein kinase (PIKK) family which has been identified as the product mutated or inactivated in ataxia telangiectasia (A-T) patients.   A key mediator of the DNA damage response is ATM kinase, which has been implicated in playing a central role in response to oxidative stress.[6-8]   Our previous studies showed that ATM mediates an instructive role in oxidative stress-induced endothelial dysfunction and premature senescence.[9]   However, the role of ATM in oxidative stress-induced Dox cardiotoxicity has remained elusive.

The heart is comprised of cardiomyocytes as well as interstitial fibroblasts in addition to other cells.   The uninjured adult murine myocardium is composed of roughly 56% myocytes, 27% fibroblasts, 7% endothelial cells and 10% vascular smooth muscle cells as well as other immune cells.[10]   Studies on the heart have historically focused in main on cardiomyocytes, but the role of cardiac fibroblasts has received increasing recent attention as pivotal functions in the maintenance of cardiac function, physiological cardiac remodeling after heart stress and pathological remodeling have been demonstrated.[11]

In the present study, we hypothesized that ATM kinase might mediate effects of oxidative stress in Dox-induced cardiotoxicity, and investigated whether this molecule, as an oxidative stress-sensing molecule, mediates the cardiotoxic effects of the oxidative agent, anthracycline. ATM indeed mediated the effects of Dox-induced cardiotoxicity, but interestingly, these effects were mediated specifically through the cardiac fibroblast as shown using conditional knockout mice.   Further, a specific antagonist against ATM, KU55933, prevented Dox-induced cardiotoxicity.   We, therefore, found that ATM is a mediator of Dox-induced cardiotoxicity,

identified cell type-specific mechanisms, and showed that ATM is a viable target for potential therapeutic exploitation.

Methods

Animal experiments

C57BL/6 mice were purchased from CLEA Japan. *Atm*-knockout mice (129S6/SvEvTac-Atm*tm1Awb*/J) were obtained from Jackson Laboratory. All generations were from matings of heterozygous parents. Age-matched eight-week-old specific pathogen free male wild-type and *Atm* homozygous knockout mice ($Atm^{-/-}$) (n=7, respectively, weighing approximately 20~25g) were used. Dox treatment was performed with a single intraperitoneal (i.p.) injection of Dox (Sigma-Aldrich) (15 mg/kg of body weight) for indicated times. C57BL/6 mice received 5mg/kg i.p. KU55933 (Tocris Bioscience) or vehicle (10%DMSO/18%Polyethylene glycol/72% sterile 5%Dextrose) as control followed by a single i.p. injection of saline or Dox (15 mg/kg of body weight). Mice were given KU55933 at -1, 2, 5 and 8 days after Dox treatment. *Fas ligand* homozygous knockout mice ($FasL^{-/-}$) (B6Smn.C3-*Fasl*^{gld}/J) were obtained from Jackson Laboratory. All generations were from matings of homozygous parents. Mice were housed under constant temperature ($23 \pm 1°C$) with a 12 hour light and 12 hour dark cycle with free access to water and chow, and sacrificed by cervical dislocation. All care and experimental procedures of animals were in accordance with the guidelines for the Care and Use of Laboratory Animals published by the National Institute of Health (NIH Publication, eighth edition, 2011). All experiments were approved by the Ethics Committee for Animal Experiments and strictly adhered to the guidelines for animal experiments of the University of Tokyo.

Conditional deletion of the *Atm* gene in cardiac fibroblasts and cardiomyocytes in mice

Homozygous *Atm*-floxed mice (*Atm^fl/fl*)[12] were crossbred with *Postn-Cre*[13] or *αMHC-Cre*[14] mice to generate fibroblast-specific *Atm*-deleted mice and cardiomyocyte-specific *Atm*-deleted mice, respectively.   Dox treatment was performed with a single i.p. injection of Dox (15 mg/kg of body weight) for indicated times.

Statistical analysis

All values are expressed as means ± s.d.   Differences between two groups were analyzed using a non-parametric test (two-tailed Mann-Whitney U-test).   Comparisons between multiple groups were done using one-way or two-way ANOVA followed by a post hoc Tukey's multiple comparisons test.   Survival curves after Dox injection were created using the Kaplan-Meier method and compared by a log-rank test.   All data were analyzed using Prism 6.0 (GraphPad Software) for Windows.   *P* values less than 0.05 were considered statistically significant.

A detailed description of the methods is provided in Supplementary Materials.

Results

ATM plays an important role in Dox-induced cardiotoxicity

Previous studies implicated oxidative stress as a major factor involved in Dox-induced cardiotoxicity.[2-5]   The DNA damage response and its main signaling pathway involving ATM has been implicated in playing a central role in mediating the actions of oxidative stress.[6-8]   We first tested the involvement of oxidative stress and ATM kinase in Dox-induced cardiotoxicity.

Oxidative stress, which was assessed by 2', 7'-dichlorofluorescein (DCF) fluorescence using

CM-H$_2$DCFDA,[15] was attenuated by a free radical scavenger N-acetyl-L-cysteine (NAC) but not

by an ATM kinase inhibitor, KU55933 (see Supplementary material online, *Figure S1A and B*).

Dox-induced ATM phosphorylation, however, was attenuated both by NAC and KU55933 (see

Supplementary material online, *Figure S1C*), thus indicating that ATM is situated downstream of

oxidative stress in Dox-induced cardiotoxicity.   To characterize the role of ATM in

Dox-induced cardiotoxicity *in vivo*, mice were treated once with Dox (15 mg/kg of body weight

by single i.p. injection) and then sacrificed after 7 days and analyzed.   Although no apparent

differences were seen in cardiac morphology (see Supplementary material online, *Figure S2A*)

between wild-type mice and *Atm* homozygous knockout mice (*Atm*$^{-/-}$), *Atm*$^{-/-}$ mice showed less

decrease in heart weight/body weight (HW/BW) ratio (*Figure 1A*), less increase in cardiac

apoptosis (*Figure 1B* and *C*), less impairment of cardiac systolic function (*Figure 1D* and *E* and

see Supplementary material online, *Table S*), less compensatory dilatation of the left ventricle

and less bradycardia (see Supplementary material online, *Figure S2B* and *Table S*).   To evaluate

the percentages of cardiomyocytes and cardiac fibroblasts in the apoptotic cell populations,

double fluorescent immunostaining of TUNEL with cardiomyocyte-specific marker (troponin T)

or cardiac fibroblast-specific marker (vimentin) were done (see Supplementary material online,

Figures S3A and *S4A*).   The results showed that approximately 20% of apoptotic cells were

cardiomyocytes whereas cardiac fibroblasts comprised approximately 80% (see Supplementary

material online, *Figures S3B* and *S4B*).   Moreover, no apparent differences were seen in the

percentages of cardiomyocytes or cardiac fibroblasts in the apoptotic cell populations between

the two groups (see Supplementary material online, *Figures S3B* and *S4B*).   Interestingly, ATM

activation was mainly detected in cardiac fibroblasts of wild-type mice on day 5 after Dox

treatment on the basis that phosphorylated ATM (ATM-S1981) was localized to cells that stained

positive for vimentin which was used as a marker to identify fibroblasts (see Supplementary

material online, *Figure S5A* and *B*).   Moreover, ATM and phosphorylated ATM induced by

Dox were more robustly expressed in cardiac fibroblasts than in cardiomyocytes *in vitro* (see

Supplementary material online, *Figure S5C*).   Fibroblasts appeared to be the key lineage

responsible for Dox-induced cardiotoxicity through ATM likely due to higher levels of

expression and activation of the protein in that cell.

Cardiac fibroblast-specific deleted *Atm* mice ameliorates depression of left ventricular

function, cardiac apoptosis and mortality in response to Dox

As ATM activation was seen mainly in fibroblasts, which suggests that its function in these cells

might contribute to the phenotypes seen in $Atm^{-/-}$ mice, the function of ATM in cardiac

fibroblasts was next investigated using cell-specific conditional knockout mice.   For this,

cardiac fibroblast-specific *Atm*-deleted mice (hereafter referred to as $Atm^{fl/fl}$;*Postn-Cre*) were

generated using $Atm^{fl/fl}$ mice[12] crossed with fibroblast-restricted *Cre* transgenic mice (*Postn-Cre)*

mice.[13]   Periostin (which is encoded by *Postn*) was selectively induced in cardiac fibroblasts

following Dox treatment (mRNA expression in *Figure 2A*, protein expression in *Figure 2B*).

Cre-recombinase activity in the fibroblasts of $Atm^{fl/fl}$;*Postn-Cre* mice was also confirmed by *in*

situ hybridization and immunohistochemistry (see Supplementary material online, *Figure S6A*

and B).   Approximately 80% of the *Atm* expression was deleted only in cardiac fibroblasts

isolated from $Atm^{fl/fl}$;*Postn-Cre* mice as compared with control $Atm^{fl/fl}$ mice 7 days after Dox

administration (see Supplementary material online, *Figure S7D* and *E*).   Western blot analysis

for ATM protein levels in the whole hearts of $Atm^{fl/fl}$;*Postn-Cre* mice showed marked reductions

in contrast to robust levels as seen in *Atm*$^{fl/fl}$ mice 7 days after Dox treatment (see Supplementary material online, *Figure S7F*).   Although no apparent differences in cardiac morphology (see Supplementary material online, *Figure S8A*) were seen between *Atm*$^{fl/fl}$;*Postn-Cre* mice and *Atm*$^{fl/fl}$ mice, *Atm*$^{fl/fl}$;*Postn-Cre* mice after Dox administration showed less decrease in HW/BW ratio (*Figure 2C*), less increase in cardiac apoptosis (*Figure 2D* and *E*), less impairment of cardiac systolic function (*Figure 2F* and *G* and see Supplementary material online, *Table S*), less compensatory dilatation of the left ventricles and less bradycardia (see Supplementary material online, *Figure S8B* and *Table S*).   However, no apparent differences were seen in the percentages of cardiomyocytes and cardiac fibroblasts in the apoptotic cell populations between the two groups (see Supplementary material online, *Figures S3C* and *S4C*).   Furthermore, survival of *Atm*$^{fl/fl}$;*Postn-Cre* mice was significantly greater than in *Atm*$^{fl/fl}$ mice 14 days after Dox treatment (*Figure 2H*).   Chronic administration of Dox (once every 7 days for 28 days) to *Atm*$^{fl/fl}$;*Postn-Cre* mice showed less cardiotoxic effects consistent with the acute model, and also less fibrosis (see Supplementary material online, *Figure S9A-C*).   Collectively, these phenotypes demonstrate that ATM expressed in cardiac fibroblasts principally mediates the effects of Dox-induced cardiotoxicity.

Cardiomyocyte-specific deleted *Atm* mice do not show different effects on Dox-induced cardiotoxicity

The function of ATM in cardiomyocytes in Dox-induced cardiotoxicity was then analyzed using cardiomyocyte-specific *Atm*-deleted mice (hereafter referred to as *Atm*$^{fl/fl}$;*αMHC-Cre*) which were generated by cross breeding *Atm*$^{fl/fl}$ mice with cardiomyocyte-restricted *Cre* transgenic mice (*αMHC-Cre*).[14]   Approximately 70% mRNA and 90% protein expression of the ATM was

deleted in cardiomyocytes (see Supplementary material online, *Figure S10A-C*). When

Atm^{fl/fl};*αMHC-Cre* mice and control *Atm^{fl/fl}* mice were subjected to Dox, there were no apparent

differences in cardiac morphology (see Supplementary material online, *Figure S11A*), decrease in

heart weight/body weight (HW/BW) ratio (*Figure 3A*), increase in cardiac apoptosis (*Figure 3B*

and *C*), percentages of cardiomyocytes and the cardiac fibroblasts in the apoptotic cell

populations (see Supplementary material online, *Figures S3D and S4D*), impairment of cardiac

systolic function (*Figure 3D* and *E* and see Supplementary material online, *Table S*),

compensatory dilatation of the left ventricle and echocardiographic parameters (see

Supplementary material online, *Figure S11B* and *Table S*) or survival (*Figure 3F*) between the

two groups, indicating that the presence nor absence of ATM in cardiomyocytes in mice affected

cardiotoxicity induced by Dox. Similar cardiotoxic effects were seen with chronic

administration of Dox (once every 7 days for 28 days) in addition to fibrosis (see Supplementary

material online, *Figure S12A-C*). Thus, cardiotoxic effects of Dox through ATM are mediated

by cardiac fibroblasts but not cardiomyocytes.

ATM mediates Dox-induced apoptosis of cardiac fibroblasts but less in cardiomyocytes *in*
vitro

Dox induced cardiac apoptosis in wild-type mice which was absent in *Atm^{-/-}* mice and

Atm^{fl/fl};*Postn-Cre* mice to a greater degree. Mechanisms *in vitro* were next addressed namely

on apoptosis which is thought to be the most direct causative factor that contributes to

Dox-induced cardiotoxicity.[16] Using neonatal rat cardiomyocytes and cardiac fibroblasts, Dox

treatment resulted in a marked increase in apoptosis of cardiac fibroblasts and cardiomyocytes,

and administration of an inhibitor of ATM, KU55933, effectively blocked cardiac fibroblast

apoptosis but only negligibly in cardiomyocytes after Dox treatment for 24 hours (*Figure 4A-D*).

These results support that cardiac fibroblasts are the key lineage responsible for causing

Dox-induced cardiotoxicity through ATM.

ATM controls expression of FasL in cardiac fibroblasts that mediate Dox-induced cardiotoxicity

Because earlier studies have suggested that there are paracrine interactions between

cardiomyocytes and fibroblasts,[17,18] we hypothesized that ATM might directly control the

expression of paracrine factors in fibroblasts.   To test this, antibody array analysis was done

which showed marked increases in apoptotic Fas ligand (FasL) after Dox treatment in

conditioned media of cardiac fibroblasts which was suppressed by KU55933 (see Supplementary

material online, *Figure S13A* and *B*).   FasL levels secreted from cardiac fibroblasts which were

isolated from adult mice after treatment with Dox were also approximately 2-fold higher than in

cardiomyocytes (see Supplementary material online, *Figure S13C*).   FasL as well as its receptor

CD95 (Fas) showed increased expression in cardiac fibroblasts in a time-dependent manner after

treatment with Dox which was less in cardiomyocytes (*Figure 5A*).   To confirm whether

apoptosis of cardiomyocytes was induced by FasL secreted from cardiac fibroblasts, Fas-Fc,

which can neutralize FasL, was added to the medium before stimulation by Dox.   Significantly,

cardiomyocytes cultured in medium conditioned by cardiac fibroblasts treated with Fas-Fc or

KU55933 showed less apoptosis when compared to cells cultured in medium conditioned by

control cells, thus indicating that FasL produced from fibroblasts can directly regulate apoptosis

of cardiomyocytes (*Figure 4E* and *F*).   Moreover, to address whether FasL is a pivotal

mediator of this mechanism *in vivo*, cardiac fibroblasts and cardiomyocytes isolated from adult

wild-type mice and *FasL*$^{-/-}$ mice were treated with Dox and then measured for apoptosis. Apoptosis of cardiac fibroblasts was significantly attenuated in *FasL*$^{-/-}$ mice compared with wild-type mice treated by Dox; however, no difference was seen in cardiomyocytes from these mice (*Figure 5B* and *C*).

Dox-induced apoptosis of cardiomyocytes from rats occurred at 24 hours as compared to mice at 48 hours.   Both similarly showed that apoptosis of cardiac fibroblasts preceded that of cardiomyocytes and was more robust (Zhan et al., unpublished observation).   Note that we focused on experimental conditions which show the involved earlier and instructive events of apoptosis as regulated through the cardiac fibroblast by ATM.   Using these differentially isolated cardiac fibroblasts and cardiomyocytes from adult wild-type and *FasL*$^{-/-}$ mice, expression of a representative apoptosis-related factor, caspase-8, was shown to be markedly increased in cardiac fibroblasts isolated from adult wild-type mice as compared to *FasL*$^{-/-}$ mice; however, there was no increase in cardiomyocytes (*Figure 5D*).   Under conditions in which Dox activated caspase 3 in cardiomyocytes, Dox also activated caspase 3 in cardiac fibroblasts. Caspase 3 was activated both in cardiomyocytes and in fibroblasts, but as caspase 8 was selectively activated in fibroblasts but not in cardiomyocytes (*Figure 5E*), involved pathways seem to differ between these cell types.   These data collectively suggest that FasL is a mediator of ATM-mediated Dox cardiotoxicity via caspase-8 *in vivo*.   These findings are consistent with results of earlier studies that showed increased susceptibility of cardiomyocytes to Fas-mediated apoptosis when damaged by Dox.[19]

KU55933, a potent and selective inhibitor of ATM, prevents Dox-induced cardiotoxicity

To test whether inhibition of ATM activation may prevent Dox-induced cardiotoxicity *in vivo*,

KU55933, a potent and selective inhibitor of ATM,[20,21] was administered to Dox-treated mice. Although there were no apparent differences in cardiac morphology (see Supplementary material online, *Figure S14A*), mice treated with KU55933 showed less decrease in HW/BW ratio (*Figure 6A*), less increase in cardiac apoptosis (*Figure 6B* and *C*), less impairment of cardiac systolic function (*Figure 6D* and *E* and see Supplementary material online, *Table S*), less compensatory dilatation of the left ventricle and less bradycardia (see Supplementary material online, *Figure S14B* and *Table S*) and mortality (*Figure 6F*). However, no apparent differences were seen in the percentages of cardiomyocytes and cardiac fibroblasts in the apoptotic cell populations between the two groups (see Supplementary material online, *Figures S3E* and *S4E*). Under these conditions, pre-treatment with KU55933 attenuated Dox-induced activation of ATM (*Figure 6G*) in the heart. Therefore, inhibition of ATM activation by KU55933 is effective in preventing Dox-induced cardiotoxicity *in vivo*.

Discussion

Anthracyclines, as represented by doxorubicin (Dox), are widely used for cancer therapy with usage limited due to its cumulative dose-dependent cardiotoxicity which leads to irreversible degenerative cardiomyopathy and heart failure in cancer patients.[1] As described in the ESC guidelines for the diagnosis and treatment of acute and chronic heart failure, anthracyclines are a major and central class of anti-cancer drugs known to harbor cardiotoxic effects. Although multiple mechanisms of Dox-induced cardiotoxicity including DNA damage, free radical formation, mitochondrial dysfunction, lipid peroxidation, altered calcium handling, and activation of pro-apoptotic signaling cascades/inhibition of survival signaling have been implicated[22] but not fully elucidated as they are likely multifactorial, substantial evidence

supports a key role for Dox-induced oxidative stress in cardiotoxicity.[23]

The present study showed that ATM mediates Dox-induced cardiotoxic effects (e.g. cardiac dysfunction, apoptosis, mortality).   Further investigations identified that effects of ATM are predominantly mediated by cardiac fibroblasts and not the cardiomyocyte through enhancing release of FasL from the fibroblast which in turn facilitates apoptosis of cardiomyocytes. Oxidative stress as sensed through ATM mainly in cardiac fibroblasts, therefore, plays an early instructive role in activation of cardiac apoptosis associated with Dox cardiotoxicity.   Our results showed that, surprisingly, cardiac fibroblasts and not cardiomyocytes, as would be expected *a priori*, not only sensed but also acted in a regulatory manner in response to the oxidative stress damage as caused by Dox.

On cell type-specific mechanisms, to our knowledge, this is the first study to have pursued the role of cardiac fibroblasts and factors in these cells in the pathological mechanisms of Dox-induced cardiotoxicity.   Investigations have shown effects of cardiomyocyte-specific ablation of factors on anthracycline cardiotoxicity including topoisomerase IIβ,[24] focal adhesion kinase,[25] breast cancer susceptibility gene II (BRCA2),[26] Survivin[27] and signal transducer and activator of transcription 3 (STAT3)[28] to mediate/promote cardiotoxic effects of Dox, and RAS-related C3 botulinus toxin substrate 1 (Rac1) to inhibit effects.[29]   Cardiac sensitization to anthracycline toxicity has also been reported in ventricular muscle-specific erbB4 knockout mouse.[30]   A study using cardiomyocyte-specific transgenic mice expressing nitric oxide synthase 3 (NOS3)[31] has further shown promoted effects on Dox-induced cardiotoxicity.   Thus, these accumulating lines of evidence have identified cardiomyocyte-mediated pathways involved in Dox-induced cardiotoxicity.   Of particular relevance to the present study, cardiomyocyte-specific ablation of p53 has been shown to not sufficiently inhibit Dox-induced

cardiotoxicity.[32]   As ATM is one of the factors lying upstream of p53, these findings are

supportive of a non-cardiomyocyte mechanism mediated by p53, likely involving but not

restricted to the described pathway through the ATM-p53 axis in the fibroblast which seems to

be only partially dependent on ATM (Zhan et al., unpublished observation).   Although the

present study suggests that ATM in cardiac fibroblasts is important in Dox-induced

cardiotoxicity, alternative mechanisms underpinning Dox-induced cardiac damage are also

feasible.   More importantly, interactions among these factors and/or pathways and their effects

on other cell types in the cardiomyocyte and cardiac fibroblast remain unknown.   Given the

cross-talk between both signaling pathway molecules and cell types in the heart through these

cells and likely other constituent cells as well, it will be important to further identify and dissect

the relative contributions and importance of individual pathways and cells to unravel the full

scope of mechanisms underlying Dox-cardiotoxicity.   The schematic diagram represents a

model of the molecular/cellular mechanism of the effect of ATM in Dox-induced cardiotoxicity

(see Supplementary material online, *Figure S15*).

Clinically, Dox-induced cardiotoxicity is a substantial drawback of anti-cancer therapy,

notably for breast cancer and lymphoma in which use of Dox is limited because of cardiotoxic

effects.   Improvements on anthracycline agents have been made such as development of newer

and less cardiotoxic agents such as epirubicin and idarubicin, and drug delivery approaches such

as use of prodrugs and liposomal delivery.   Further, a variety of cardioprotective agents to

prevent Dox-induced cardiotoxicity have been tried including statins, coenzyme Q10, l-carnitine,

carvedilol, N-acetyl-l-cysteine (NAC), combinations of vitamins E and C with NAC, digoxin,

enalapril, phenethylamines, deferoxamine, ethylenediaminetetraacetic acid (EDTA), superoxide,

dismutase and monohydroxyethylrutoside.   At present, only the iron-chelating EDTA derivative,

dexrazoxane, which is thought to chelate and reduce the number of metal ions complexed with the anthracyclines and therefore reduce formation of superoxide radical formation, is presently recommended by the ESC for use as a cardioprotective agent for patients receiving these anti-cancer agents.[33,34] KU55933, which inhibited ATM activity and thus was protective against cardiotoxic effects of Dox in the present study, was developed and pursued as a possible anti-cancer drug, in particular in patients with breast cancer. Nonetheless, we have identified a novel cell-specific molecular signaling pathway which might be potentially exploitable for therapeutic purposes.

Conceptually, combined use of anti-cancer agents that inhibit ATM to prevent cardiotoxicity by Dox might allow for effective methods to overcome the limitations of the latter while allowing combined effect of the two anti-cancer agents with possible use of lesser individual dosages through combinatorial sensitization effects.[35,36] Cell-type specific targeted therapy (e.g. fibroblast-specific ATM antagonism), possibly in combination with those targeting other pathways involved in Dox-induced cardiotoxicity (e.g. cardiomyocyte-specific pathways), might pose further therapeutic possibilities as lineage-restricted targets. With newer anti-cancer agents such as trastuzumab, sorafenib and sunitinib also showing cardiotoxic effects but with lesser known mechanisms, similar approaches may have general and wide applicability.

Study Limitations

The findings of the study are limited by the criteria of the employed technical approaches. One is that *αMHC-Cre*-expressing mice are leaky in expression in cardiomyocytes (approximately 30% expression) and are somewhat a hypomorph rather than null deletion which limits the accuracy of the statements made using these mice although this mouse is the best available at this

time.   Experiments using these mice warrant revisitation once better and improved mice become available.   Variability in response to Dox according to animal species was another limitation, specifically different apoptotic responses between rat and mice derived cells as used in the present study.   Importantly, results were consistent but differed in quantitative aspects (e.g reduced Dox-induced apoptotic effects on cardiomyocytes isolated from murine cardiomyocytes).   There are also limitations on the involved mechanisms.   Fas-mediated regulation was the center of investigation in our studies, but cross-talk with p53 in both an ATM dependent and independent manner as well as relative contribution needs to be further delineated *in vivo* in subsequent studies (e.g. fibroblast-specific FasL knock-out mice to delineate role and contribution of the ATM-p53 pathway).

Conflict of interest: None declared.

References

1. Takemura G, Fujiwara H. Doxorubicin-induced cardiomyopathy from the cardiotoxic mechanisms to management. *Prog Cardiovasc Dis.* 2007; **49**: 330-352.

2. Lefrak EA, Pitha J, Rosenheim S, Gottlieb JA. A clinicopathologic analysis of adriamycin cardiotoxicity. *Cancer.*1973; **32**: 302-314.

3. Gilladoga AC, Manuel C, Tan CT, Wollner N, Sternberg SS, Murphy ML. The cardiotoxicity of adriamycin and daunomycin in children. *Cancer.* 1976; **37**:1070-1078.

4. Bristow MR, Thompson PD, Martin RP, Mason JW, Billingham ME, Harrison DC. Early anthracycline cardiotoxicity. *Am J Med.* 1978; **65**:823-832.

5. Von Hoff DD, Layard MW, Basa P, Davis HL Jr, Von Hoff AL, Rozencweig M, Muggia FM. Risk factors for doxorubicin-induced congestive heart failure. *Ann Intern Med.* 1979; **91**:710-717.

6. Ito K, Hirao A, Arai F, Matsuoka S, Takubo K, Hamaguchi I, Nomiyama K, Hosokawa K, Sakurada K, Nakagata N, Ikeda Y, Mak TW, Suda T. Regulation of oxidative stress by ATM is required for self-renewal of haematopoietic stem cells. *Nature.* 2004; **431**:997-1002.

7. Barzilai A, Rotman G, Shiloh Y. ATM deficiency and oxidative stress: a new dimension of defective response to DNA damage. *DNA Repair (Amst).* 2002; **1**:3-25.

8. Shiloh, Y. ATM and related protein kinases: safeguarding genome integrity. *Nat Rev Cancer*. 2003; **3**:155-168.

9. Zhan H, Suzuki T, Aizawa K, Miyagawa K, Nagai R. Ataxia telangiectasia mutated (ATM)-mediated DNA damage response in oxidative stress-induced vascular endothelial cell senescence. *J Biol Chem.* 2010; **285**:29662-29670.

10. Banerjee I, Fuseler JW, Price RL, Borg TK, Baudino TA. Determination of cell types and numbers during cardiac development in the neonatal and adult rat and mouse. *Am J Physiol Heart Circ Physiol.* 2007; **293**:H1883-1891.

11. Fujiu K, Nagai R. Contributions of cardiomyocyte-cardiac fibroblast-immune cell interactions in heart failure development. *Basic Res Cardiol.* 2013; **108**:357.

12. Lee Y, Shull ER, Frappart PO, Katyal S, Enriquez-Rios V, Zhao J, Russell HR, Brown EJ, McKinnon PJ. ATR maintains select progenitors during nervous system development. *EMBO J.* 2012; **31**:1177-1189.

13. Takeda N, Manabe I, Uchino Y, Eguchi K, Matsumoto S, Nishimura S, Shindo T, Sano M, Otsu K, Snider P, Conway SJ, Nagai R. Cardiac fibroblasts are essential for the adaptive response of the murine heart to pressure overload. *J Clin Invest.* 2010; **120**:254-265.

14. Agah R, Frenkel PA, French BA, Michael LH, Overbeek PA, Schneider MD. Gene recombination in postmitotic cells. Targeted expression of Cre recombinase provokes cardiac-restricted, site-specific rearrangement in adult ventricular muscle in vivo. *J Clin Invest.* 1997; **100**:169-179.

15. Wang H, Joseph JA. Quantifying cellular oxidative stress by dichlorofluorescein assay using microplate reader. *Free Radic Biol Med.* 1999; **27**:612-616.

16. Minotti G, Menna P, Salvatorelli E, Cairo G, Gianni L. Anthracyclines: molecular advances and pharmacologic developments in antitumor activity and cardiotoxicity. *Pharmacol Rev.* 2004; **56**:185-229.

17. Baudino TA, Carver W, Giles W, Borg TK. Cardiac fibroblasts: friend or foe? *Am J physiol Heart Circ Physiol.* 2006; **291**:H1015-1026.

18. Manabe I, Shindo T, Nagai R. Gene expression in fibroblasts and fibrosis: involvement in

cardiac hypertrophy. *Circ Res.*2002; **91**:1103-1113.

19. Yamaoka M, Yamaguchi S, Suzuki T, Okuyama M, Nitobe J, Nakamura N, Mitsui Y, Tomoike H. Apoptosis in rat cardiac myocytes induced by Fas ligand: priming for Fas-mediated apoptosis with doxorubicin. *J Mol Cell Cardiol.* 2000; **32**:881-889.

20. Croxford JL, Tang ML, Pan MF, Huang CW, Kamran N, Phua CM, Chng WJ, Ng SB, Raulet DH, Gasser S. ATM-dependent spontaneous regression of early Emu-myc-induced murine B-cell leukemia depends on natural killer and T cells. *Blood.* 2013; **121**:2512-2521.

21. Batey MA, Zhao Y, Kyle S, Richardson C, Slade A, Martin NM, Lau A, Newell DR, Curtin NJ. Preclinical evaluation of a novel ATM inhibitor, KU59403, in vitro and in vivo in p53 functional and dysfunctional models of human cancer. *Mol Cancer Ther.* 2013; **12**:959-967.

22. Sawyer DB, Peng X, Chen B, Pentassuglia L, Lim CC. Mechanisms of anthracycline cardiac injury: can we identify strategies for cardioprotection? *Prog Cardiovasc Dis.* 2010; **53**:105-113.

23. Deavall DG, Martin EA, Horner JM, Roberts R. Drug-induced oxidative stress and toxicity. *J Toxicol.* 2012; **2012**:645460.

24. Zhang S, Liu X, Bawa-Khalfe T, Lu LS, Lyu YL, Liu LF, Yeh ET. Identification of the molecular basis of doxorubicin-induced cardiotoxicity. *Nat Med.* 2012; **18**:1639-1642.

25. Cheng Z, DiMichele LA, Rojas M, Vaziri C, Mack CP and Taylor JM. Focal adhesion kinase antagonizes doxorubicin cardiotoxicity via p21 (Cip1.). *J Mol Cell Cardiol.* 2014; **67**:1-11.

26. Singh KK, Shukla PC, Quan A, Desjardins JF, Lovren F, Pan Y, Garg V, Gosal S, Garg A, Szmitko PE, Schneider MD, Parker TG, Stanford WL, Leong-Poi H, Teoh H, Al-Omran M and Verma S. BRCA2 protein deficiency exaggerates doxorubicin-induced cardiomyocyte

apoptosis and cardiac failure. *J Biol Chem.* 2012; **287**:6604-14.

27. Levkau B, Schafers M, Wohlschlaeger J, von Wnuck Lipinski K, Keul P, Hermann S, Kawaguchi N, Kirchhof P, Fabritz L, Stypmann J, Stegger L, Flogel U, Schrader J, Fischer JW, Hsieh P, Ou YL, Mehrhof F, Tiemann K, Ghanem A, Matus M, Neumann J, Heusch G, Schmid KW, Conway EM and Baba HA. Survivin determines cardiac function by controlling total cardiomyocyte number. *Circulation.* 2008; **117**:1583-93.

28. Jacoby JJ, Kalinowski A, Liu MG, Zhang SS, Gao Q, Chai GX, Ji L, Iwamoto Y, Li E, Schneider M, Russell KS and Fu XY. Cardiomyocyte-restricted knockout of STAT3 results in higher sensitivity to inflammation, cardiac fibrosis, and heart failure with advanced age. *Proc Natl Acad Sci U S A.* 2003; **100**:12929-34.

29. Ma J, Wang Y, Zheng D, Wei M, Xu H and Peng T. Rac1 signalling mediates doxorubicin-induced cardiotoxicity through both reactive oxygen species-dependent and -independent pathways. *Cardiovasc Res.* 2013; **97**:77-87.

30. Vasti C, Witt H, Said M, Sorroche P, Garcia-Rivello H, Ruiz-Noppinger P and Hertig CM. Doxorubicin and NRG-1/erbB4-Deficiency Affect Gene Expression Profile: Involving Protein Homeostasis in Mouse. *ISRN Cardiol.* 2012; **2012**:745185.

31. Neilan TG, Blake SL, Ichinose F, Raher MJ, Buys ES, Jassal DS, Furutani E, Perez-Sanz TM, Graveline A, Janssens SP, Picard MH, Scherrer-Crosbie M and Bloch KD. Disruption of nitric oxide synthase 3 protects against the cardiac injury, dysfunction, and mortality induced by doxorubicin. *Circulation.* 2007; **116**:506-14.

32. Feridooni T, Hotchkiss A, Remley-Carr S, Saga Y, Pasumarthi KB. Cardiomyocyte specific ablation of p53 is not sufficient to block doxorubicin induced cardiac fibrosis and associated cytoskeletal changes. PLoS One. 2011; **6**:e22801.

33. Van Dalen EC, Caron HN, Dickinson HO, Kremer LC. Cardioprotective interventions for cancer patients receiving anthracyclines. *Cochrane Database Syst Rev.* 2011; CD003917.pub4

34. Hasinoff BB, Herman EH. Dexrazoxane: how it works in cardiac and tumor cells. Is it a prodrug or is it a drug? *Cardiovasc Toxicol.* 2007; **7**: 140-144.

35. Khalil HS, Tummala H, Hupp TR, Zhelev N. Pharmacological inhibition of ATM by KU55933 stimulates ATM transcription. *Exp Biol Med (Maywood).* 2012; **237**:622-634.

36. Curtin NJ. DNA repair dysregulation from cancer driver to therapeutic target. *Nat Rev Cancer.* 2012; **12**:801-817.

Figure legends

Figure 1   Regulation of Dox-induced cardiotoxicity by ATM.   *Atm*^{-/-} and wild-type (WT) mice were subjected to a single i.p. injection of saline or Dox (15 mg/kg of body weight) for 7 days to induce cardiotoxicity.   (*A*) Heart weight/body weight (HW/BW) ratio (n=7 per group).   (*B* and *C*) Dox-induced cardiac apoptosis as assessed by terminal deoxynucleotidyl transferase-mediated dUTP nick-end labeling (TUNEL) staining.   Immunoreactivity was visualized with diaminobenzidine (brown).   Hematoxylin was used as nuclear stain (blue).   Arrows indicate representative TUNEL-positive cardiac cells (*B*).   Scale bar, 50 μm.   Apoptosis index (percentage of TUNEL-positive nuclei) was calculated as total TUNEL-positive nuclei/total nuclei × 100 (%).   Apoptosis index of cardiac cells were plotted (n=3 per group, total of 18 visual fields) (*C*).   (*D* and *E*) Echocardiographic analysis (n=5 per group).   M-mode echocardiographic tracings (*D*) and left ventricular fractional shortening (LVFS) (*E*) of mice treated with saline or Dox.   Results are expressed as means ± s.d.; *P<0.05; **P<0.01; NS: not significant, by two-way ANOVA followed by a post hoc Tukey's multiple comparisons test.

Figure 2   Absence of Dox-induced cardiotoxicity in fibroblast-specific *Atm*-deleted mice.   *Atm*^{fl/fl} and *Atm*^{fl/fl};*Postn-Cre* mice were subjected to a single i.p. injection of saline or Dox (15 mg/kg of body weight) for 7 days to induce cardiotoxicity.   (*A*) Expression of periostin in cardiac fibroblasts and cardiomyocytes.   Cardiac fibroblasts and cardiomyocytes isolated from neonatal mice were treated with 1 μM of Dox for 12 or 24 hours and then expression of periostin was assessed using real-time PCR.   (*B*) Expression of periostin in cardiac fibroblasts and cardiomyocytes after treatment with Dox as assessed by Western blot analysis.   Cardiac

fibroblasts and cardiomyocytes isolated from neonatal mice were treated with 1 μM Dox for indicated times.   Cells were lysed and subjected to Western blot analysis with indicated antibodies.   GAPDH was used as loading control.   (*C*) Heart weight/body weight (HW/BW) ratio (n=7 per group).   (*D* and *E*) Dox-induced cardiac apoptosis as assessed by TUNEL staining.   Immunoreactivity was visualized with diaminobenzidine (brown).   Hematoxylin was used as nuclear stain (blue).   Arrows indicate representative TUNEL-positive cardiac cells (*D*). Scale bar, 50 μm.   Apoptosis index (percentage of TUNEL-positive nuclei) was calculated as total TUNEL-positive nuclei/total nuclei $\times$ 100 (%).   Apoptosis index of cardiac cells were plotted (n=3 per group, total of 18 visual fields) (*E*).   (*F* and *G*) Echocardiographic analysis (n=5 per group).   M-mode echocardiographic tracings (*F*) and LVFS (*G*) of mice treated with saline or Dox.   Results are expressed as means ± s.d.; **P<0.01; NS: not significant, by two-way ANOVA followed by a post hoc Tukey's multiple comparisons test.   (*H*) Kaplan-Meier survival analysis of *Atm*$^{fl/fl}$ (n=25) and *Atm*$^{fl/fl}$*;Postn-Cre* (n=31) mice 2 weeks after treatment with Dox.   **P<0.01 by log-rank test.

Figure 3   Dox-induced cardiotoxicity in cardiomyocyte-specific *Atm*-deleted mice.   *Atm*$^{fl/fl}$ and *Atm*$^{fl/fl}$*;αMHC-Cre* mice were subjected to a single i.p. injection of saline or Dox (15 mg/kg of body weight) to for 7 days induce Dox-induced cardiotoxicity.   (*A*) Heart weight/body weight (HW/BW) ratio (n=7 per group).   (*B* and *C*) Dox-induced cardiac apoptosis as assessed by TUNEL staining.   Immunoreactivity was visualized with diaminobenzidine (brown). Hematoxylin was used as nuclear stain (blue).   Arrows indicate representative TUNEL-positive cardiac cells (*B*).   Scale bar, 50 μm.   Apoptosis index (percentage of TUNEL-positive nuclei) was calculated as total TUNEL-positive nuclei/total nuclei $\times$ 100 (%).   Apoptosis index of

cardiac cells were plotted (n=3 per group, total of 18 visual fields) (*C*). (*D* and *E*)

Echocardiographic analysis (n=5 per group). M-mode echocardiographic tracings (*D*) and

LVFS (*E*) of mice treated with saline or Dox. Results are expressed as means ± s.d.; **P<0.01;

NS: not significant, by two-way ANOVA followed by a post hoc Tukey's multiple comparisons

test. (*F*) Kaplan-Meier survival analysis of *Atm^{fl/fl}* (n=28) and *Atm^{fl/fl};αMHC-Cre* (n=29) mice 2

weeks after treatment with Dox. Note that there are no significant (NS) differences between

Atm^{fl/fl} and *Atm^{fl/fl};αMHC-Cre* mice.

Figure 4 Regulation of Dox-induced apoptosis by ATM in cardiac fibroblasts *in vitro*. (*A-D*)

Effects of ATM inhibitor (KU55933) on Dox-induced apoptosis of cardiac fibroblasts (CF) or

cardiomyocytes (CM) were assessed by TUNEL staining. Cardiac fibroblasts or

cardiomyocytes isolated from neonatal rats were pre-treated with 1 μM or 10 μM KU55933 for

30 minutes followed by administration of 1 μM Dox for 24 hours and then immunostained for

TUNEL assay (brown). Hematoxylin was used as nuclear stain (blue). Arrows indicate

representative TUNEL-positive cardiac fibroblasts (*A*) or cardiomyocytes (*C*). Scale bar, 100

μm. Apoptosis index (percentage of TUNEL-positive nuclei) was calculated as total

TUNEL-positive nuclei/total nuclei × 100 (%). Apoptosis index of cardiac fibroblasts (*B*) or

cardiomyocytes (*D*) were plotted. (*E* and *F*) Effects of conditioned medium from cardiac

fibroblasts on Dox-induced cardiomyocyte apoptosis were assessed by TUNEL staining.

Cardiomyocytes isolated from neonatal rats were incubated for another 24 hours with

conditioned medium prepared from cardiac fibroblasts pre-treated with KU55933 (an inhibitor of

ATM, 10 μM) or Fas-Fc (neutralizing agent of FasL, 10 μg/ml) 30 minutes followed by

administration of 1 μM Dox for 24 hours, and then immunostained for TUNEL assay (brown) in

cardiomyocytes.   Arrows indicate representative TUNEL-positive cardiomyocytes (*E*).   Scale

bar, 100 μm.   Apoptosis index (percentage of TUNEL-positive nuclei) was calculated as total

TUNEL-positive nuclei/total nuclei $\times$ 100 (%).   Apoptosis index of cardiac cells were plotted

(*F*).   Results are expressed as means ± s.d. (n=3 per group, total of 9 visual fields); **P<0.01;

NS: not significant, by one-way ANOVA followed by a post hoc Tukey's multiple comparisons

test.   Pre Tx: Pre-treatment; KU1: KU55933 1 μM; KU10: KU55933 10 μM; Sup. From CF:

Conditioned medium prepared from cardiac fibroblasts.   Ctrl: Pre Tx-free and Dox-free.

Figure 5   Mechanism of FasL in regulating Dox cardiotoxicity.   (*A*) Dox-induced FasL and

CD95 expression as assessed by Western blot analysis.   Cardiac fibroblasts and cardiomyocytes

isolated from neonatal mice were incubated in 1 μM Dox for indicated times.   Cells were lysed

and subjected to Western blot analysis with indicated antibodies (n=3 per group).   (*B* and *C*)

Effects of FasL on Dox cardiotoxicity *in vivo*.   Cardiac fibroblasts (*B*) and cardiomyocytes (*C*)

isolated from adult WT or *FasL*$^{-/-}$ mice were treated with 1 μM Dox for 24 hours and then

assessed using the Cell Death Detection ELISA^{Plus} kit.   Results are expressed as means ± s.d.

(n=3 per group); **P<0.01; NS: not significant, by two-way ANOVA followed by a post hoc

Tukey's multiple comparisons test.   (*D*) Effects of FasL on the apoptosis-related factor

caspase-8 *in vivo*.   Cardiac fibroblasts and cardiomyocytes isolated from adult WT or *FasL*$^{-/-}$

mice were treated with 1 μM Dox for indicated times and then assessed by Western blot analysis

(n=3 per group).   (*E*) Dox-induced caspase-8 and caspase-3 expressions as assessed by Western

blot analysis.   Cardiac fibroblasts and cardiomyocytes isolated from neonatal mice were

incubated in 1 μM Dox for indicated times.   Cells were lysed and subjected to Western blot

analysis with indicated antibodies (n=3 per group).   GAPDH was used as loading control.

Figure 6 Effects of ATM inhibitor, KU55933 (KU), on Dox-induced cardiotoxicity *in vivo*

after 2 weeks. (*A*) Heart weight/body weight (HW/BW) ratio (n=5 per group). (*B* and *C*)

Dox-induced cardiac apoptosis as assessed by TUNEL staining. Immunoreactivity was

visualized with diaminobenzidine (brown). Hematoxylin was used as nuclear stain (blue).

Arrows indicate TUNEL-positive cardiac cells (*B*). Scale bar: 50 μm. Apoptosis index

(percentage of TUNEL-positive nuclei) was calculated as total TUNEL-positive nuclei/total

nuclei $\times$ 100 (%). Apoptosis index of cardiac cells were plotted (n=3 per group, total of 18

visual fields) (*C*). (*D* and *E*) Echocardiographic analysis (n=5 per group). M-mode

echocardiographic tracings (*D*) and LVFS of mice (*E*) treated with saline or Dox, or KU55933 +

Dox. Results are expressed as means ± s.d.; **P<0.01 by one-way ANOVA followed by a post

hoc Tukey's multiple comparisons test. (*F*) Kaplan-Meier survival analysis of C57BL/6 mice 2

weeks after treatment with Dox (n=19) and C57BL/6 mice treatment with KU55933 + Dox

(n=19). **P<0.01 by log-rank test. (*G*) Expression of ATM (S1981) and ATM examined by

Western blot analysis. GAPDH was used as loading control.
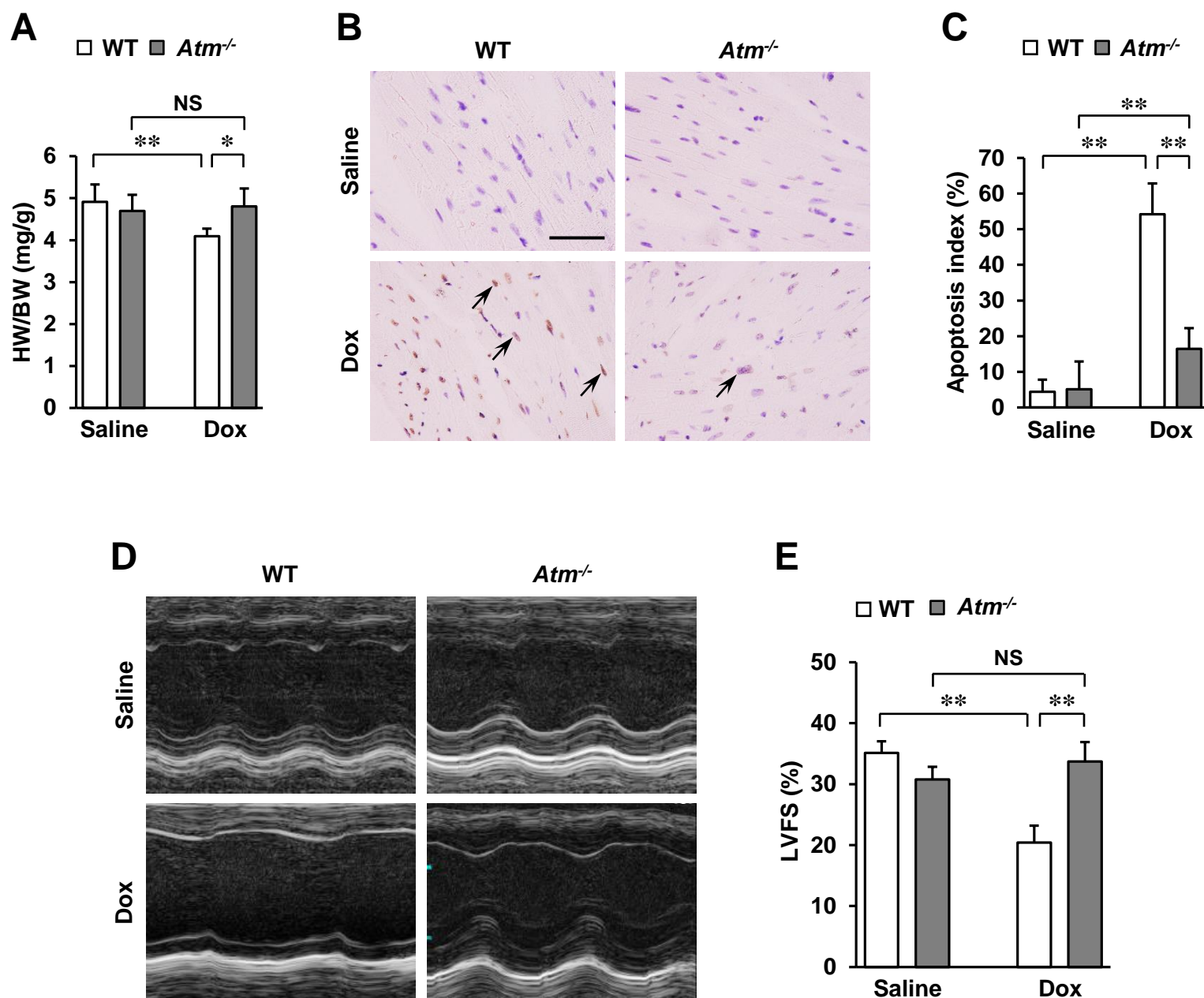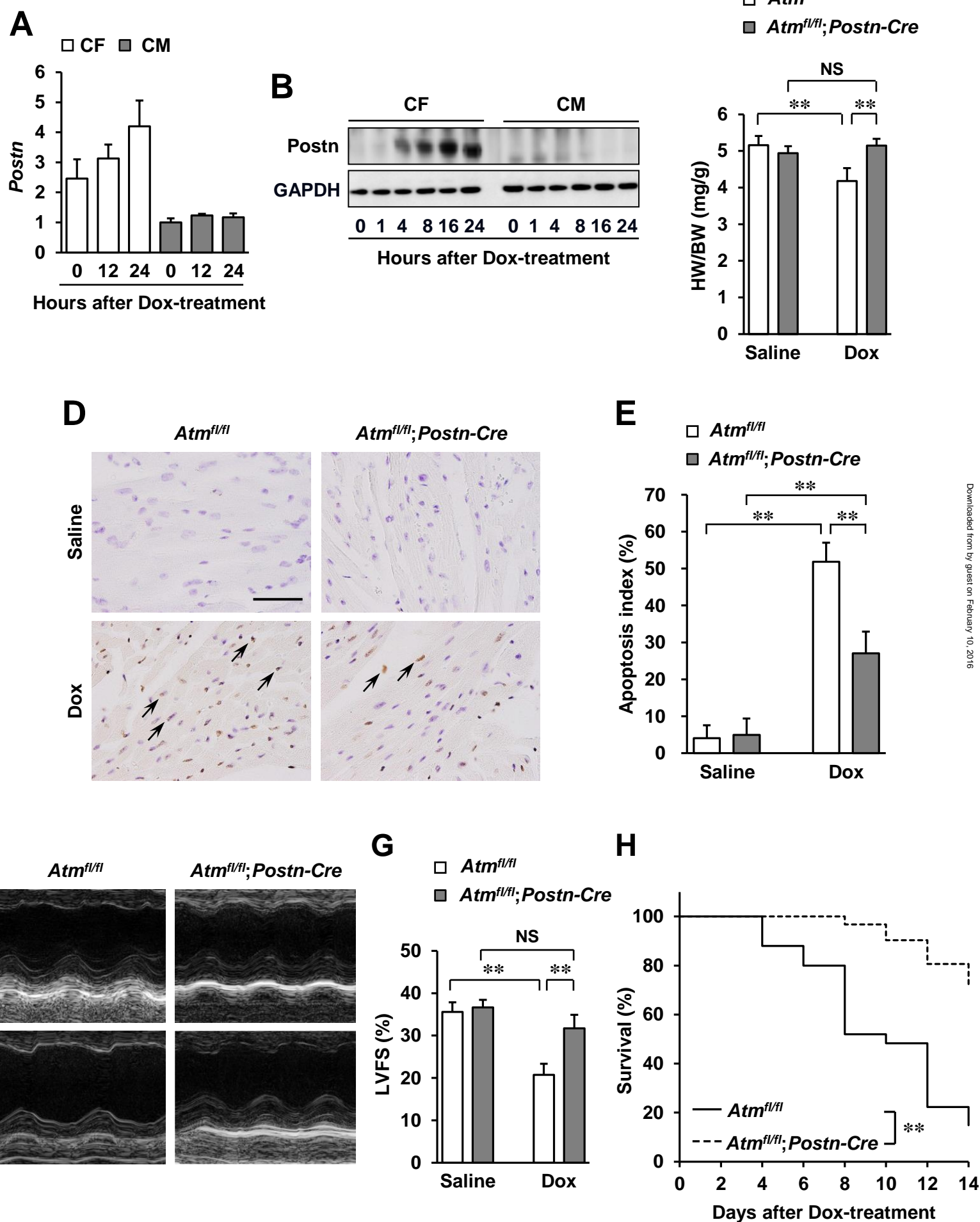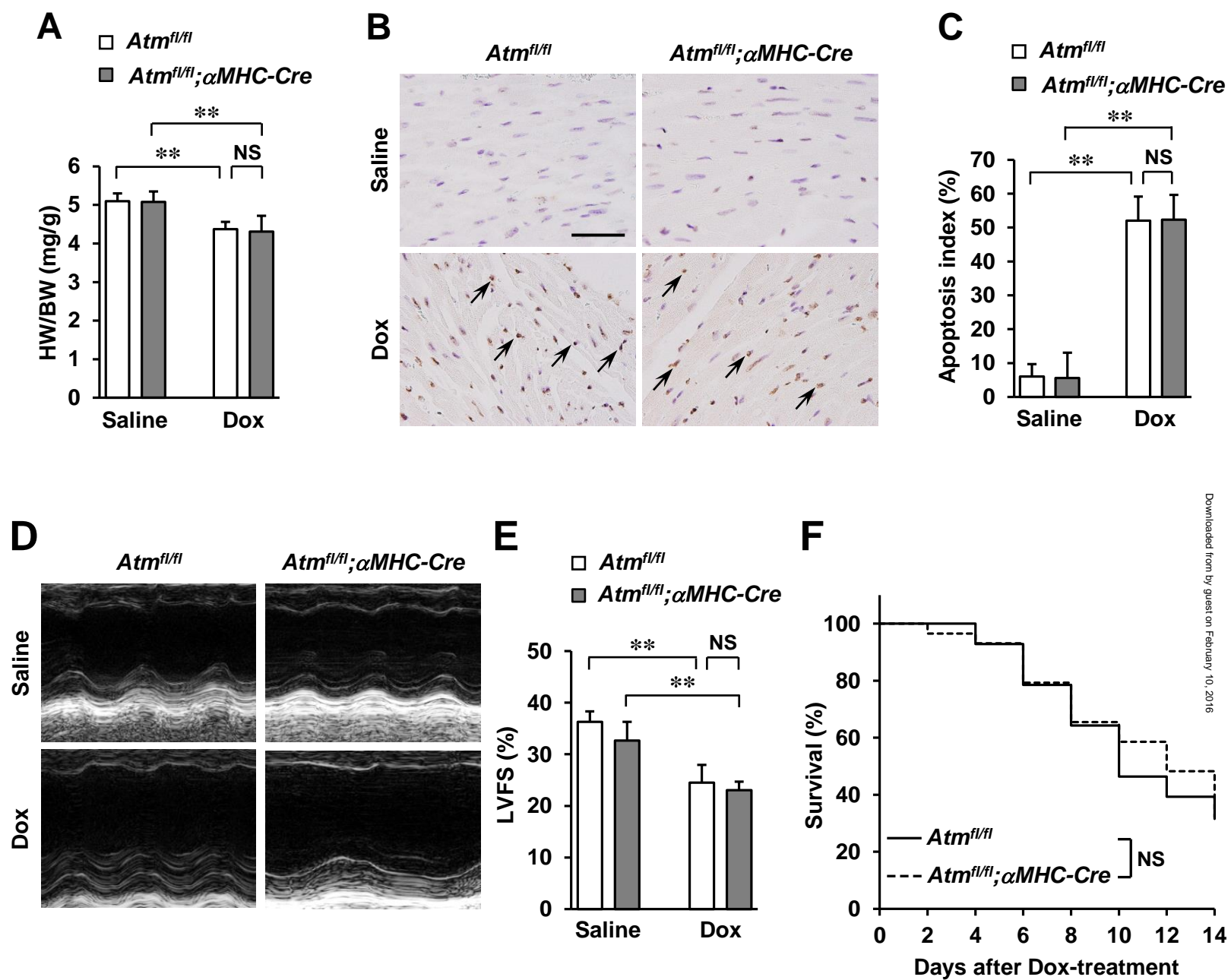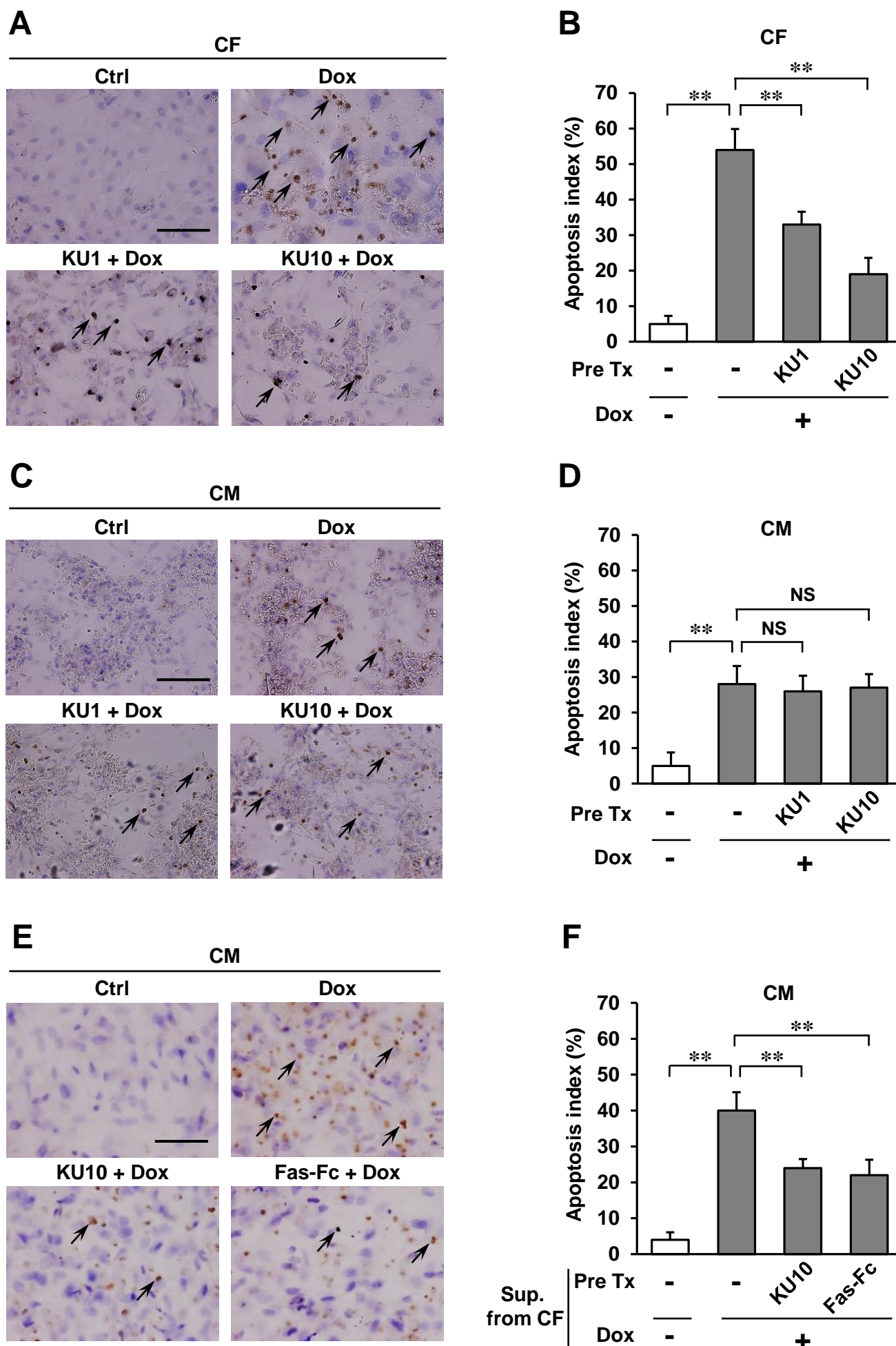
Figure 1

A

B

C

D

E

Figure 2

Figure 3

Figure 4

Figure 5

A

CF   CM

FasL — 40 kDa

CD95 — 45 kDa

GAPDH — 37 kDa

0 1 4 8 16 24   0 1 4 8 16 24

Hours after Dox-treatment

B

CF

□ WT ■ FasL⁻/⁻

Apoptosis (Fold increase)

** **

NS

0 24 0 24

Hours after Dox-treatment

C

CM

□ WT ■ FasL⁻/⁻

Apoptosis (Fold increase)

NS   NS

NS

0 24 0 24

Hours after Dox-treatment

D

CF   CM

WT   FasL⁻/⁻   WT   FasL⁻/⁻

Caspase 8 — 43 kDa

GAPDH — 37 kDa

0 4 8 16 24 0 4 8 16 24   0 4 8 16 24 0 4 8 16 24

Hours after Dox-treatment   **Hours after Dox-treatment**

E

CF   CM

Caspase 8 — 43 kDa

Caspase 3 — 17 kDa

GAPDH — 37 kDa

0 12 24   0 12 24

Hours after Dox-treatment

Figure 6

A

B

| Saline | Dox | KU + Dox |

C

D

| Saline | Dox | KU + Dox |

E

F

G

ATM-S1981	– 370 kDa
ATM	– 370 kDa
GAPDH	– 37 kDa

| KU | - | - | + | + |
| Dox | - | + | + | - |